Chemical Grafting of Biphenyl Self-Assembled Monolayers on Ultrananocrystalline Diamond

Simon Q. Lud,[†] Marin Steenackers,[‡] Rainer Jordan,*,[‡] Paola Bruno,[§]
Dieter M. Gruen,[§] Peter Feulner,[‖] Jose A. Garrido,*,[†] and Martin Stutzmann[†]

Contribution from the Walter Schottky Institut, Technische Universität München,
Am Coulombwall 3, 85748 Garching, Germany, Lehrstuhl für Makromolekulare Stoffe,
Technische Universität München, Lichtenbergstrasse 4, 85747 Garching, Germany,
Materials Science Department, Argonne National Laboratory, Argonne, Illinois 60439, and
Physics Department E20, Technische Universität München, James-Franck-Strasse,
85748, Garching, Germany

Received August 7, 2006; E-mail: garrido@wsi.tum.de; rainer.jordan@ch.tum.de

Abstract: We have investigated the formation of self-assembled monolayers (SAMs) of 4′-nitro-1,1-biphenyl-4-diazonium tetrafluoroborate (NBD) onto ultrananocrystalline diamond (UNCD) thin films. In contrast to the common approach to modify diamond and diamond-like substrates by electrografting, the SAM was formed from the saturated solution of NBD in acetonitrile by pure chemical grafting. Atomic force microscopy (AFM), X-ray photoelectron spectroscopy (XPS), cyclic voltammetry (CV), and near edge X-ray absorption fine structure spectroscopy (NEXAFS) have been used to verify the direct covalent attachment of the 4′-nitro-1,1-biphenyl (NB) SAM on the diamond substrate via stable C−C bonds and to estimate the monolayer packing density. The results confirm the presence of a very stable, homogeneous and dense monolayer. Additionally, the terminal nitro group of the NB SAM can be readily converted into an amino group by X-ray irradiation as well as electrochemistry. This opens the possibility of in situ electrochemical modification as well as the creation of chemical patterns (chemical lithography) in the SAM on UNCD substrates and enables a variety of consecutive chemical functionalization for sensing and molecular electronics applications.

Introduction

Ultrananocrystalline diamond (UNCD) has received much attention for both biosensing applications and electron transfer investigations.[1,2] There are several reasons that suggest that UNCD has a great potential as a material for amperometric biosensors. First of all, conductive diamond is considered an excellent electrode material for electrochemistry, with very low background current and the largest electrochemical potential window of all solids. Although UNCD electrodes do not match the extreme performance of single and polycrystalline diamond electrodes, they possess other advantages such as low production cost and the scalability to large area deposition. Moreover, it has been reported that the stability of DNA films grafted onto diamond surfaces is far superior to the stability of the same films grafted onto more common substrates such as gold or SiO_2.[2,3] Furthermore, it has also been demonstrated that complex biomolecules such as proteins remain active after grafting to UNCD surfaces.[4] Finally, UNCD is almost inert toward complex biological environments, and it is often used in the field of biomedical sensors, implants, and coatings for biologically functionalized micromechanical system (bioMEMS) devices.[5] A stable organic functionalization with, for example, conjugated aromatic moieties of diamond surfaces provides both high electron-transfer rate constants and proximal biochemical binding sites and constitutes an attractive approach for designing novel and well-defined interfaces for such applications.

The chemical modification of diamond or diamond-like surfaces is difficult due to the almost inert nature of the substrate. In the last years, however, several research groups successfully applied the electrochemically induced grafting of aryl diazonium derivatives on diamond[6] and other carbon surfaces as well as semiconductors and various metals. The current state of the art in this field was recently reviewed by Pinson and Podvorica.[7] One major drawback of this approach is the reported formation of multilayers with the ongoing grafting procedure due to the transfer of electrons through the growing film.[8−10]

[†] Walter Schottky Institut, Technische Universität München.
[‡] Lehrstuhl für Makromolekulare Stoffe, Technische Universität München.
[§] Argonne National Laboratory.
[‖] Physics Department E20, Technische Universität München.

(1) Carlisle, J. A.; Auciello, O. *Electrochem. Soc. Interface* **2003**, *12*, 28.
(2) Yang, W. S.; Auciello, O.; Butler, J. E.; Cai, W.; Carlisle, J. A.; Gerbi, J.; Gruen, D. M.; Knickerbocker, T.; Lasseter, T. L.; Russell, J. N., Jr.; Smith, L. M.; Hamers, R. J. *Nat. Mater.* **2002**, *1*, 253−257.
(3) Wenmackers, S.; Christiaens, P.; Daenen, M.; Haenen, K.; Nesladek, M.; van deVen, M.; Vermeeren, V.; Michiels, L.; Ameloot, M.; Wagner, P. *Phys. Status Solidi* **2005**, *202*, 2212.

(4) Härtl, A.; Schmich, E.; Garrido, J. A.; Hernando, J.; Catharino, S. C. R.; Walter, S.; Feulner, P.; Kromka, A.; Steinmuller, D.; Stutzmann, M. *Nat. Mater.* **2004**, *3*, 736.
(5) Auciello, O.; Birrell, J.; Carlisle, J. A.; Gerbi, J. E.; Xiao, X. C.; Peng, B.; Espinosa, H. D. *J. Phys.: Condens. Matter.* **2004**, *16*, 539.
(6) Wang, J.; Firestone, M. A.; Auciello, O.; Carlisle, J. A. *Langmuir* **2004**, *26*, 11450.
(7) Pinson, J.; Podvorica, F. *Chem. Soc. Rev.* **2005**, *34*, 429.
(8) Kariuki, J. K.; McDermott, M. T. *Langmuir* **2001**, *17*, 5947.
(9) Anariba, F.; DuVall, S. H.; McCreery, R. L. *Anal. Chem.* **2003**, *75*, 3837.

More recently, the pure chemical grafting of aryl diazonium salts onto carbon black[11] and other surfaces (Si,[12,13] GaAs,[12] Au,[14] Pd,[12] Cu,[15] Fe[16]) has been reported.[7] The proposed mechanism of the grafting reaction involves a spontaneous electron transfer between the substrate and the diazonium compound and might be otherwise similar to the electrografting reaction route.[7] The advantage of this procedure is its simplicity, the substrates are submerged in a solution (mostly acetonitrile) of the aryl diazonium compound, and no electrochemical equipment is needed. In addition, as the chemically inert diamond surface is expected to have low surface contamination, the diazonium compounds do not have to compete with other impurities during the grafting process. In order to enable a defined self-assembled monolayer by chemical grafting, the mesogen of the surface active molecule is crucial to provide an additional intralayer ordering of the organic monolayer. Due to our experience with SAMs of biphenyl thiols on gold and silver substrates,[17,18] we selected the stable 4′-nitro-1,1-biphenyl-4-diazonium tetrafluoroborate (NBD) for the chemical grafting onto UNCD substrates. The biphenyl moiety proved to be an excellent mesogen for the establishment of highly ordered and densely packed SAMs,[17,19] the terminal 4′-position can be varied over a broad range of functionalizations that also allow consecutive reactions[19] such as the surface-initiated polymerizations.[21,22] Moreover, the mesogen is conjugated and enables an electrochemical coupling between the distal surface and the proximal function and give rise to unique optical properties.[23] Finally, the biphenyl is rigid and does not allow surface reconstruction[20] as observed in common alkane-based SAMs.

In this report, we investigate the reaction of NBD and hydrogenated UNCD surfaces, which results in a homogeneous self-assembled monolayer of 4′-nitro-1,1-biphenyl (NB). X-ray photoelectron spectroscopy investigations, and cyclic voltammetry studies were used to investigate the presence and packing density of the monolayer film. Furthermore, reduction of the terminal 4′-nitro group of the NB SAM into a functional amino group of the resulting 4′-amino-1,1-biphenyl (AB) SAM was performed by X-ray irradiation under ultra-high vacuum conditions as well as electrochemically in physiological environment. The conversion was followed by XPS and NEXAFS studies. The free, residual amino group of the final AB SAM opens the

Scheme 1 [a]
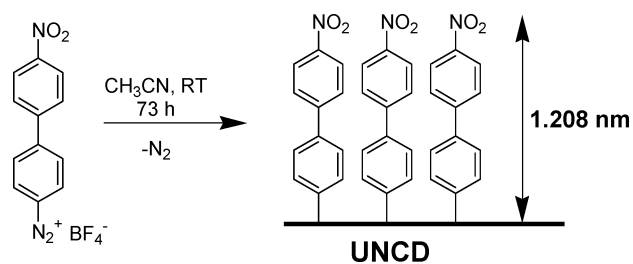
[a] Reaction of the NBD with UNCD to form the SAM of NB along with the calculated thickness of the SAM as reported by McCreery and co-workers.[9]

possibility of attaching proteins onto the otherwise inert diamond surface.[24,25]

Materials and Methods

Reagents and Substrates. For AFM measurements, commercially available (ElementSix Advancing Diamond Ltd., UK) polished (rms < 1 nm, measured in an area of 5 × 5 μm) polycrystalline diamond samples with the dimensions of $5 \times 5 \times 0.5$ mm^3 were used. All other samples employed were about 1 μm thick ultrananocrystalline diamond CVD layers grown by microwave-assisted chemical vapor deposition on 600-μm-thick p-doped silicon {100} substrates. Conductive UNCD films were grown from a $N_2/Ar/CH_4$ gas mixture with 20% nitrogen in the gas phase.[26] All reagents were of the highest grade available and were used directly without further purification. Ultrapure deionized water of resistivity greater than 18 MΩ·cm from a Milli-Q water purification system (Millipore, Bedford, MA) was used to prepare all aqueous solutions.

Synthesis of 4′-Nitro-1,1-biphenyl-4-diazonium Terafluoroborate (NBD). NBD was synthesized from 4′-nitro-1,1-biphenyl-4-amino (ABCR, Germany) following a procedure by McCreery and co-workers.[27] The product was purified by reprecipitation (cold acetonitrile/cold dry ether) and characterized by ^{1}H NMR spectroscopy and stored at −20 °C. Yield: 72% (colorless powder). Directly before every further use, NBD was reprecipitated from dry ether.

Diamond Functionalization

UNCD Substrates. For the XPS and NEXAFS measurements, a wafer of UNCD was diced into 12 × 12 mm^2 pieces. The surfaces were cleaned by sequential rinsing in acetone, 2-propanol, and water prior to insertion into an oxygen plasma system (Giga-Etch 100-E, TePla AG, Germany), where they were treated for 300 s with an oxygen plasma (300 W load coil power; pressure of 1.5 mbar). For subsequent hydrogenation, samples were transferred into a vacuum chamber, for hydrogenation by atomic hydrogen generated by a hydrogen gas flow of 150 standard cm^3 over a hot (2000 °C) tungsten filament, placed at a distance of 4 cm from the substrate. During the process, the sample temperature (700 °C) was determined with a thermocouple.

NB SAM Preparation. The freshly hydrogenated diamond surface was immersed into a degassed and saturated solution of NBD in approximately 0.5 mL of acetonitrile and stirred for 72 h. During the reaction, a gradual color change of the clear reaction solution to a bright yellow and finally to a deep orange color was observed. In some cases the reaction time was varied by some hours but did not affect the herein reported spectroscopic results. The proposed reaction is displayed in Scheme 1.[6] Finally, the surface was cleaned by thorough ultrasonifi-

(10) Allongue, P.; Henry de Villeneuve, C.; Cherouvrier, G.; Cortès, R. Bernard, M.-C. *J. Electroanal. Chem.* **2003**, *550−551*, 162.
(11) Cooke, J. M.; Galloway, C. P.; Bissell, M. A.; Adams, C. E.; Yu, M. C.; Belmont, J. A.; Amici, R. M. U.S. Patatent 6,110,9994A, 2003 (to Cabot Corporation).
(12) Stewart, M. P.; Maya, F.; Kosynkin, D. V.; Dirk, S. M.; Stapleton, J. J.; McGuiness, C. L.; Allara, D. L.; Tour, J. M. *J. Am. Chem. Soc.* **2004**, *126*, 370.
(13) Chen, B.; Flatt, A. K.; Jian, H.; Hudson, J. L.; Tour, J. M. *Chem. Mater.* **2005**, *17*, 4832.
(14) Laforgue, A.; Addou, T.; Belanger, D. *Langmuir* **2005**, *21*, 6855.
(15) Hurley, B. L.; McCeery, R. L. *J. Electrochem. Soc.* **2004**, *151*, B252−B259 and references therein.
(16) Chaussé, A.; Chehimi, M. M.; Karsi, N.; Pinson, J.; Podvorica, F.; Vautrin-Ul, C. *Chem. Mater.* **2002**, *14*, 392.
(17) Kang, J. F.; Ulman, A.; Liao, S.; Jordan, R.; Yang, G.; Liu, G.-Y. *Langmuir* **2001**, *17*, 95.
(18) Ulman, A.; Kang, J. F.; Shnidman, Y.; Liao, S.; Jordan, R.; Choi, G.-Y.; Zaccaro, J.; Myerson, A. S.; Rafailovich, M.; Sokolov, J.; Fleischer, C. *Rev. Mol. Biotechnol.* **2000**, *74*, 175.
(19) Kang, J. F.; Ulman, A.; Jordan, R. *Langmuir* **1998**, *14*, 3983.
(20) Kang, J. F.; Ulman, A.; Jordan, R. *Langmuir* **1999**, *15*, 2095.
(21) Jordan, R.; Ulman, A.; Kang, J. F.; Rafailovich, M. H.; Sokolov, J. *J. Am. Chem. Soc.* **1999**, *121*, 1016.
(22) Schmelmer, U.; Jordan, R.; Geyer, W.; Gölzhäuser, A.; Eck, W.; Grunze, M.; Ulman, A. *Angew. Chem.* **2003**, *115*, 577; *Angew. Chem. Int. Ed.* **2003**, *42*, 559.
(23) Kang, J. F.; Jordan, R.; Ulman, A.; Kurth, D. G. *Langmuir* **1999**, *15*, 5555.

(24) Wang, J.; Carlisle, J. A. *Diamond Relat. Mater.* **2006**, *15*, 279.
(25) Gu, H. R.; Ng, Z. Y.; Deivaraj, T. C.; Su, X. D.; Loh, K. P. *Langmuir* **2006**, *22*, 3929.
(26) Bhattacharyya, S.; Auciello, O.; Birrell, J.; Carlisle, J. A.; Curtiss, L. A.; Goyette, A. N.; Gruen, D. M.; Krauss, A. R.; Schlueter, J.; Sumant, A.; Zapol, P *Appl. Phys. Lett.* **2001**, *79*, 1441.
(27) Solak, A. O.; Eichorst, L. R.; Clark, W. J.; McCreery, R. L. *Anal. Chem.* **2003**, *75*, 296.

cation for several minutes in acetonitrile, ethyl acetate and ethanol successively.

Electrode Preparation. The functionalized diamond was mounted onto a ceramic strip with a single-sided titanium—gold layer produced by evaporation. A small quantity of silver paste was applied to establish the contact between the metal pads on the ceramic and the silicon backside of the sample. Then, a single-component silicone rubber (Scrintec 901) was used as a glob top to the pads and the outer regions of the functionalized diamond specimen. After the complete assembly, the electrode was rinsed with water.

Instrumentation

Atomic Force Microscopy (AFM). AFM measurements were performed under ambient conditions in tapping mode with a Nanoscope IIIa (Veeco Instruments, Santa Barbara, CA). Images were taken at a resolution of 512×512 data points. Section and localized depth analysis was performed using the raw data. The measurement of the monolayer height was performed following the protocol of McCreery and co-workers.[9] First a $1 \times 1\ \mu m^2$ large section was scratched into the NB modified UNCD substrate at a deflection setpoint of 15 V in full contact mode. The same region was then imaged at an area of $3.4 \times 3.4\ \mu m^2$ in tapping mode. The scanned data were then analyzed by the section analysis of individual scan lines ($n = 10$) crossing the trench as well as by the local depth analysis option by choosing larges possible areas within the scratched region and the intact surface around the trench (see Figure 1). The scratching experiment and data analysis were repeated several times to ensure reproducibility and for better statistics.

X-ray Photoelectron Spectroscopy. Photoelectron spectroscopy was carried out under UHV conditions either using a homemade XPS System equipped with an Al Kα X-ray source (1486.6 eV) or at the undulator beamline U49/2-PGM-1 of the synchrotron light source BESSY II in Berlin, Germany. The spectra were recorded with an 80° incident X-ray angle and an 80° takeoff angle with respect to the surface normal (angle of incidence at BESSY: 7°, exit angle 90°). Survey scans were collected over the kinetic energy range of 50−1100 eV with 50 eV pass energy. Higher resolution scans were made over a range of 25 eV around the peaks of interest with 20 eV pass energy for quantitative measurements of the binding energy and atomic concentration. Spectra were calibrated using the Au 4f peak from an Au substrate. NEXAFS experiments were also carried out at U49/2-PGM beamline in the partial electron yield.

Cyclic Voltammetry. Electrochemical measurements were accomplished in a one-compartement cell using a three electrode setup with a Ag/AgCl reference electrode (MetroOhm AG, Germany) and a platinum wire counter electrode. Solutions were deoxygenated with nitrogen prior to electrochemical measurements. Cyclic voltammetry was performed using a Parstat 2263 potentiostat (Princeton Applied Research, U.S.A.). Before the recording of the cycles, the sample was allowed to equilibrate at the starting potential during 30 s.

Results and Discussion

Grafting and AFM Analysis of the Monolayer. First, polished and freshly hydrogenated polycrystalline diamond was submerged in a saturated solution of NBD in acetonitrile for 72 h and then thoroughly cleaned from ungrafted material by excessive ultrasonic treatment. The proposed reaction is depicted in Scheme 1.

In order to verify the formation of a monolayer of NB on the diamond surface, the modified polycrystalline diamond substrate was subjected to a scratch experiment as recently described by McCreery and co-workers.[9] At high depletion forces, a small section of the surface was "scanned" in full contact mode to remove grafted molecules but leave the hard diamond substrate intact. Imaging of the intentional applied defect and analysis
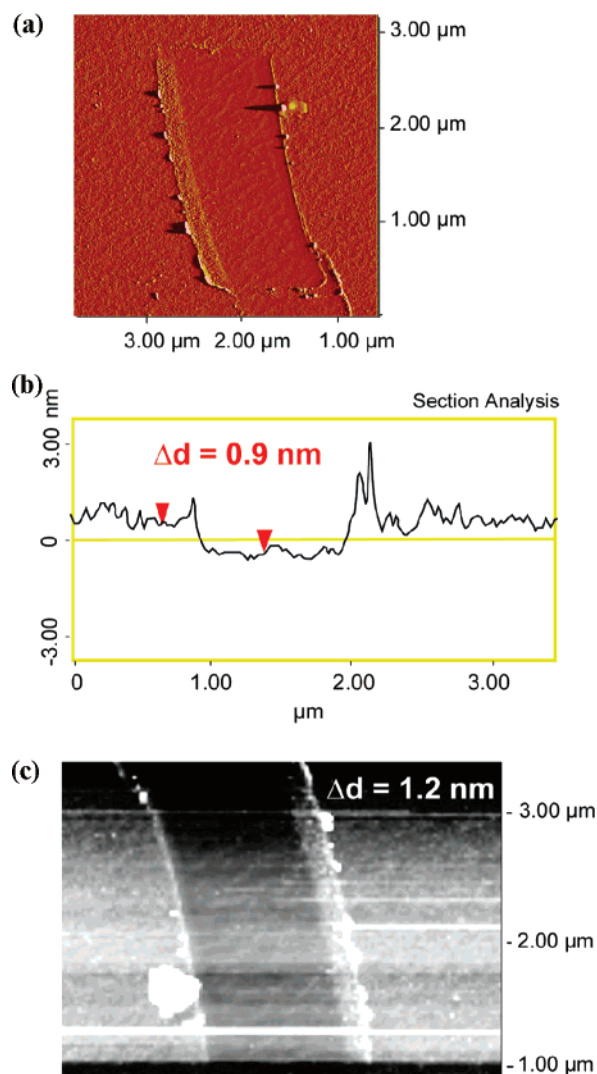
Figure 1. (a) Phase image of the AFM scan (10th scan) in tapping mode of a trench, fabricated in full contact mode by intentional remove of the NB SAM from the UNCD substrate using a high depletion setpoint of 15 V. Visible is the removed material at the rim. (b) Representative example of a line profile spanning the trench. The height difference was measured to be 0.9 ± 0.4 nm. (c) Height image of a detail of the trench used for the localized depth analysis. The selected areas in the scratched area and at the intact NB monolayer is indicated by the two boxes. The localized depth analysis gave an average height difference of 1.2 ± 0.2 nm.

of the height difference between the scratched and intact surface gave a difference of $\Delta d = 0.9 \pm 0.4$ nm (section analysis of individual scan lines) or $\Delta d = 1.2 \pm 0.2$ nm for the monolayer thickness. Taking into account the uncertainty of the measurement (e.g., tip-induced deformation of the monolayer) and variation of Δd due to the surface roughness of the substrate, the experimental thickness values of the modification is in excellent agreement with the theoretical height of a SAM of NB with a perpendicular orientation of the biphenyl molecules with respect to the surface plane (Scheme 1). Moreover, investigation of several areas of the modified polycrystalline diamond showed a homogeneous topography and no indications of the formation of multilayers as reported for the electrochemical induced modification of carbon surfaces. From AFM inspection only, the formation of a homogeneous ultrathin film with a thickness corresponding to the molecular dimension of NB can be stated.
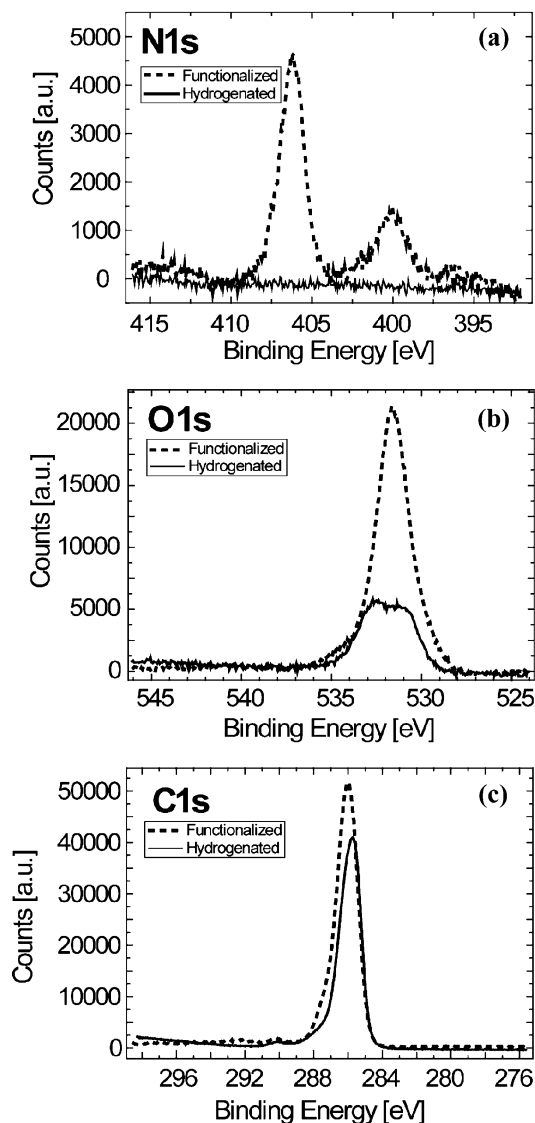
Figure 2. (a) N1s XPS spectra of a NB-functionalized diamond surface as compared to a reference sample of hydrogenated UNCD. Details of the O1s (b) and C1s (c) core level spectra of the same two samples.

X-ray Photoelectron Spectroscopy of the NB Monolayer. For closer analysis, extensive XPS measurements were performed on UNCD substrates. The XPS overview spectra (not shown) of a native hydrogenated as well as a NB functionalized surface contain carbon, nitrogen, and oxygen core level peaks. The latter two appear with higher intensity for the NB-modified diamond sample, which indicates the presence of a nitro group containing molecule at the surface. Figure 2a shows two N1s spectra of UNCD samples before and after the grafting reaction of NB. In the N1s region the amino group exhibits a binding energy peak at 400 eV, while the nitro sites appear around 406 eV. These assignments are in agreement with earlier reports.[28]

The nitrogen to carbon (N/C) ratio was calculated by the area of both peaks taking the sensitivity factors for nitrogen and carbon into account. For the calculation of the expected N/C ratio of a dense monolayer on a diamond substrate, the inelastic mean free paths for electrons with the corresponding kinetic energy are a key parameter. For surface coverage quantification,

(28) Eck, W.; Stadler, V.; Geyer, W.; Zharnikov, M.; Golzhauser, A.; Grunze, M. *Adv. Mater.* **2000**, *12*, 805.

Table 1. XPS Atom Ratios of Nitrogen, Oxygen, and Carbon together with the Derived Surface Coverage of the 4′-Nitro-1,1-biphenyl Monolayer

	chemical shift	binding energy (eV)	ratio to C1s substrate peak	packing density[a] (%)
nitrogen N1s	N—H, N•	399.9	0.11	70
	N—O	406.1		
oxygen O1s	O—N	531.7	0.25	80
carbon C1s	C—O, C=O	286.9	0.19	
	C—C	286.0	0.81	

[a] Calculated packing density of the NB monolayer with respect to the bulk crystal of 4′-nitro-1,1-biphenyl-4-amine.

we assume that the overall emission intensity I_A of a given XPS peak follows a Beer−Lambert law for the escaping electrons:

$$I_A = \int_0^\infty I_{ML} \exp^{(-u \cdot x)} dx = \frac{I_{ML}}{\mu}$$

Here, μ is the scattering coefficient or inverse mean free path, I_{ML} represents the intensity of a monolayer (approximately 0.28 nm in ultrananocrystalline diamond),[29] and the integration is along an axis parallel to the surface normal. For samples consisting of different elements, sensitivity factors have to be taken into account. For a densely packed monolayer of NB, an N/C ratio of 0.14 is expected, evaluated from X-ray charge density data of a 4′-nitro-1,1-biphenyl-4-amine crystal.[30] Table 1 shows the N/C and O/C atomic ratios calculated from the XPS spectra as described above. The measured N/C ratio of 0.11 of the functionalized surface calculates to a packing density of the molecules in the monolayer of approximately 70% with respect to the bulk crystal or to a surface grafting density of $\Gamma = 4.6 \times 10^{-10}$ mol/cm^2. For comparison, the electrochemical grafting reaction of NB yields a surface coverage of 6.5×10^{-10} mol/cm^2 on glassy carbon and 1.6×10^{-10} mol/cm^2 on the basal plane of highly ordered pyrolytic graphite (HOPG).[31] Furthermore, the O1s spectra of the functionalized UNCD surface exhibits a peak at 532 eV, which is related to the presence of a nitro group. For this peak, the ratio to the C1s carbon peak was determined to be 0.25, since two oxygen atoms contribute to the signal intensity, the packing density of the NB monolayer can be estimated to be 80% with respect to the bulk crystal and calculated to a grafting density of $\Gamma = 5.3 \times 10^{-10}$ mol/cm^2.

Figure 3, panels a and b, shows the high-resolution C1s XPS spectra of the NB-modified UNCD along with the native, hydrogenated UNCD substrate for comparison. The C1s spectrum of the hydrogenated sample could be deconvoluted into four peaks (80% Gaussian and 20% Lorentzian) at different binding energies. From this fit it is possible to accurately determine the relative percentages of carbon in various binding states: C=O, C—O, sp^2, and sp^3. The dominant peak (285.6 ± 0.1 eV) of the C1s band corresponds to the sp^3 hybridized carbon bonds; the peak located at slightly lower binding energy (285.1 ± 0.1 eV) can be assigned to the sp^2 hybridized carbon (see Table 2).

The component around 286.2 ± 0.1 eV can be assigned to the C—O group,[32] and the peak at the highest binding energy

(29) Zapol, P.; Sternberg, M.; Curtiss, L. A.; Frauenheim, Th.; Gruen, D. M. *Phys. Rev. B* **2002**, *65*, 045403.
(30) Volkov, A.; Wu, G.; Coppens, P. *J. Synchrotron Radiat.* **1999**, *6*, 1007.
(31) Liu, Y. C.; McCreery, R. L. *J. Am. Chem. Soc.* **1995**, *117*, 11254.
(32) Xu, T.; Yang, S.; Lu, J.; Xue, Q.; Li, J.; Guo, W. M; Sun, Y. *Diamond Relat. Mater.* **2001**, *10*, 1441.
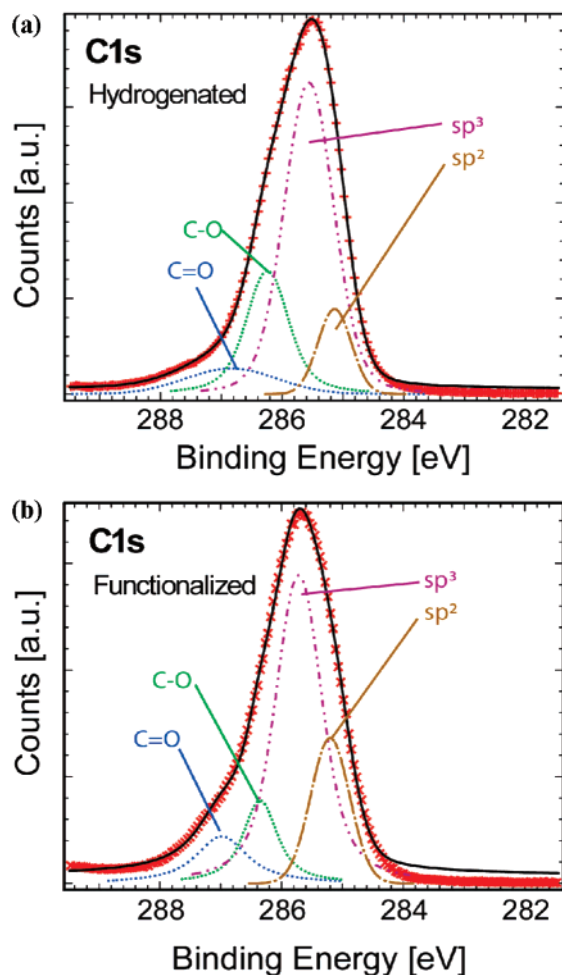
Figure 3. C1s spectra of a hydrogenated sample (a) and a functionalized sample. (b) A fit deconvolution into four different carbon binding states is shown.

Table 2. C1s Spectra Deconvolution of the C1s Region of a Hydrogenated and the NB-Functionalized UNCD Surface

peak	C–C sp	C–C sp^3	C–O	C=O
		Hydrogenated		
binding energy (eV)	285.1	285.6	286.2	286.8
composition	0.07	0.63	0.18	0.12
		NB-Functionalized		
binding energy (eV)	285.2	285.7	286.3	287.0
composition	0.18	0.57	0.14	0.11

of 286.8 ± 0.1 eV originates from C=O.[33] The sp^2/sp^3 ratio of the hydrogenated UNCD is in the order of 0.11, which is in good agreement with values for ultrananocrystalline diamond reported elsewhere.[1] The carbon–oxygen emission peak indicates a contribution potentially originated from grain boundaries impurities. The splitting of the C1s emission peak is in very good agreement with results reported by Popov et al.[34]

The XPS spectra of the functionalized diamond surface are displayed in Figure 3b. The peak attributed to the sp^2 carbon has significantly increased by a factor of 1.6 due to the presence of the phenyl rings on the surface. The sp^3 peak is still observable since the electron escape depth in carbon is about 3

(33) Wilson, J. I. B.; Walton, J. S.; Beamson, G. *J. Electron Spectrosc. Relat. Phenom.* **2001**, *121*, 183.
(34) Popov, C.; Kulisch, W.; Boycheva, S.; Yamamoto, K.; Cecone, G.; Koga, Y. *Diamond Relat. Mater.* **2004**, *13*, 2071.
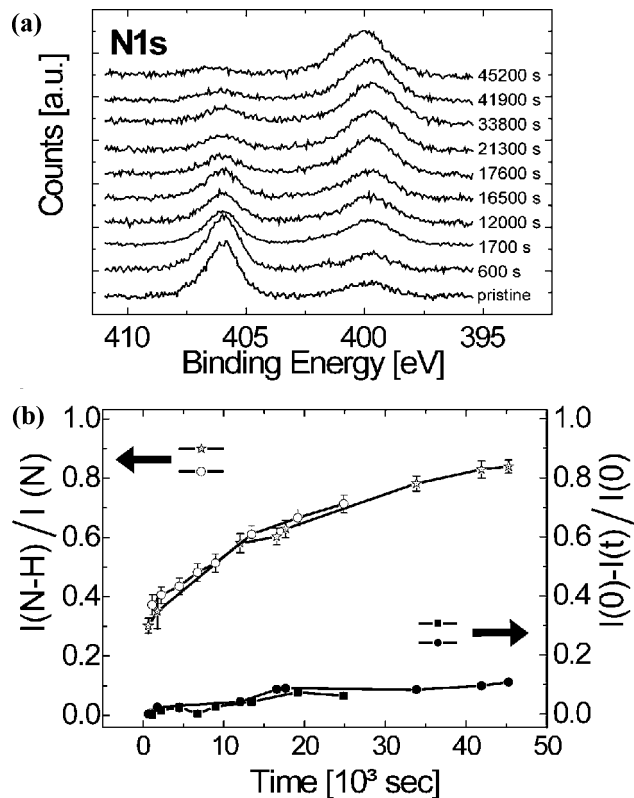
Figure 4. (a) Subsequently recorded nitrogen 1s emission spectra of a NB-modified diamond surface for increasing X-ray irradiation times. Longer radiation time induces a change in the chemical shift of the nitrogen photoelectron emission from an N–O to N–H binding configuration. (b) Dependence of the nitrogen peak area vs irradiation time of two individual samples. The left y-axis displays the fraction of nitrogen in the N–H chemical shift; the right axis shows the loss of N1s intensity to the initial intensity.

nm[35] for electrons with a kinetic energy of about 1200 eV, thus larger than the thickness of the NB monolayer. The sp^2/sp^3 peak intensity ratio can be used for an independent quantitative analysis of the formed NB monolayer. The increase of sp^2 bonded carbon is consistent with a densely packed SAM of NB and calculates to a packing density of 60% with respect to the density of a bulk crystal.

Radiation-Induced Chemical Conversion. During the XPS measurements we observed that prolonged irradiation with X-rays significantly changes the peak intensities in the N1s region (Figure 4a). The N1s peak at higher binding energy corresponding to oxygen-bonded nitrogen decreases, while a simultaneous increase of the amino-related nitrogen peak at 399.9 eV is observable. This suggests that an irradiation-induced reduction of the functional end group of the organic monolayer occurs. In fact, the (electron) irradiation-induced chemical change of 4′-nitro-1,1-biphenylthiol monolayers on gold to its 4′-amino derivative and simultaneous cross-linking of the biphenyl moieties within the SAM[36] has been reported earlier by Eck et al.[28] and is used for the so-called "chemical lithography"[28,37] and for substrate nanostructuring.[38] Similar

(35) Tanuma, S.; Powell, C. J.; Penn, D. R. *Surf. Interface Anal.* **2004**, *36*, 1–14.
(36) Eck, W.; Küller, A.; Grunze, M.; Völkel, B.; Gölzhäuser, A. *Adv. Mater.* **2005**, *17*, 2583.
(37) Gölzhäuser, A.; Eck, W.; Geyer, W.; Stadler, V.; Weimann, T.; Hinze, P.; Grunze, M. *Adv. Mater.* **2001**, *13*, 806.
(38) Küller, A.; Eck, W.; Stadler, V; Geyer, W.; Gölzhäuser, A. *Appl. Phys. Lett.* **2003**, *82*, 3776.

findings were also made with X-ray irradiation of SAMs of aromatic nitro compounds bound to SiO$_2$ by Preece and co-workers.[39] Even though X-rays interact only slightly with matter, they generate primary and secondary electrons, which can induce a cross-linking. Furthermore the ionizing radiation can further generate radicals within the organic film that are stable under UHV conditions. This can give rise to C–C or C≡C bond scission, followed by chain–chain cross-linking of neighboring ring carbon atoms.[27] This process can include a release of hydrogen for the reduction of the adjacent nitro group. The amount of nitrogen with the chemical shift of nitrogen bonded in an amino configuration is displayed in Figure 4b. The fraction of amino-related nitrogen increases steadily with the X-ray radiation time. The continuous radiation during the XPS analysis of the modified diamond surface thus gives rise to the conversion of the terminal NO$_2$ to NH$_2$ moieties of the NB SAM. The NH$_2$ content increases from 20% to 85%. At the same time, the total amount of nitrogen bonded to the surface decreases only slightly (right *y*-axis in Figure 4b), and the total loss of nitrogen in the NB SAM is about 10% after 12 h of constant irradiation.

NEXAFS Studies. NEXAFS experiments are particularly suitable to investigate the presence of sp^2 hybridized carbon on the modified diamond surface. As depicted in Figure 5a, the NEXAFS spectrum of a NB-functionalized UNCD substrate shows combined signals from both the grafted phenyl moiety and the diamond. The strong peak (A) at 285.1 eV photon energy is assigned to the C1s → π^* resonance, corresponding to sp^2 C–C bonds of the surface bonded biphenyl moieties, which is absent in the UNCD hydrogenated reference sample spectrum shown in Figure 5b (A′). The peak of low intensity (B) at 287.5 eV can be attributed to the C1s → σ^* transitions of C–H-bonded carbon located on the phenyl rings of the biphenyl monolayer. Again, no corresponding feature can be detected for the nonmodified surface (B′). Spectral features at 292 eV (C, C′) with several small peaks are associated with the C1s → σ^* resonance of C–C bonds.[40]

NEXAFS has also been used to investigate the X-ray induced nitro to amino conversion. Figure 5c represents a set of nitrogen K edge excitation spectra of the NB monolayer on UNCD. The soft X-ray synchrotron radiation (500.0 eV) gradually alters the intensity and ratio of the different resonances in N1s region with radiation time. Two low-energy N1s → σ^* (N–H) resonances are observed at 397.8 eV (A″) and at 399.6 eV (B″).[41] Increasing exposure, increases the intensity of these two σ^* resonances, indicating the transformation process of the nitro group. As expected, the intensity of the two resonances at 404 eV (C″) and at 413 eV (D″) originating from the N1s → π^* (N–O) and N1s → σ^* (N–O) transitions[42] decrease with longer irradiation times. Thus, the NEXAFS results as presented in Figure 5 are in very good agreement with the above-discussed XPS data (Figure 4) and corroborate our findings.

Electrochemical Characterization. An independent quantitative analysis of the NB SAM on diamond was carried out by electrochemical methods. Here, the terminal nitro group is

(39) Mendes, P.; Belloni, M.; Ashworth, M.; Hardy, C.; Nikitin, K.; Fitzmaurice, D.; Critchley, K.; Evans, S.; Preece, J. *ChemPhysChem.* **2003**, *4*, 884.
(40) Hoffman, A.; Laikhtman, A.; Comtet, G.; Hellner, L.; Dujardin, G. *Phys. Rev. B* **2000**, *62*, 12, 8446.
(41) La, Y.-H.; Jung, Y. J.; Kang, T.-H.; Ihm, K.; Kim, K. J.; Kim, B.; Park, J. W. *Langmuir* **2003**, *19*, 9984.
(42) Weiss, K.; Wöll, C.; Johannsmann, D. *J. Chem. Phys.* **2000**, *113*, 11297.
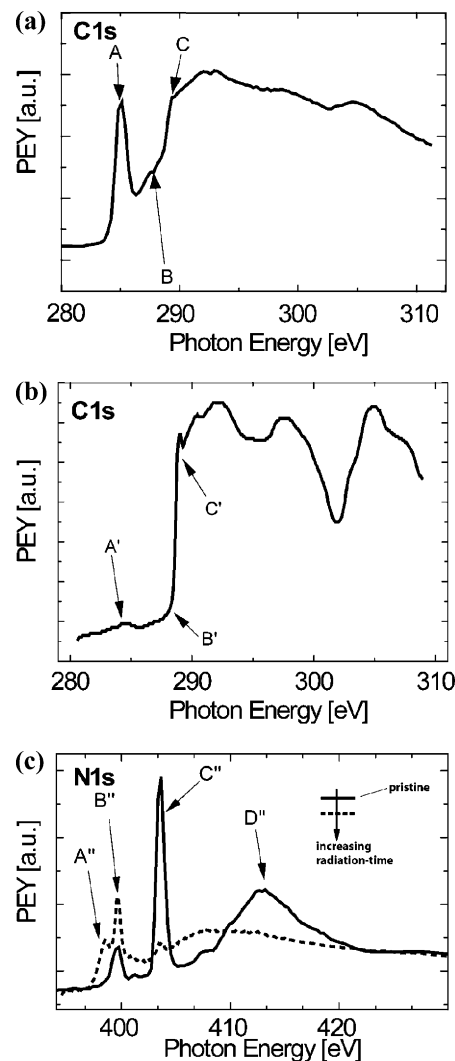
Figure 5. (a) Photon yield C1s NEXAFS absorption spectra of a biphenyl grafted UNCD sample. An intense C1s → π^* resonances, feature A, occurs in the absorption spectra, originating from the π-bonded carbon atoms within the phenyl ring. (b) NEXAFS spectra of a hydrogenated UNCD sample. (c) NEXAFS spectra recorded at the N1s edge. The following subsequently recorded spectra show a radiation induced peak change of the σ^* and π^* resonances.

known to be a suitable electroactive group. The reductive conversion of the nitro group of the NB monolayer to the corresponding amino-terminated SAM can be achieved by electrochemistry, which allows, for example, an in situ conversion of the SAM and immediate coupling of compounds additionally added to the electrolyte. This transformation was monitored by measuring the cyclic voltammogram of a freshly functionalized UNCD electrode.

Figure 6a shows a prominent cathodic peak in the first scan at a potential of −1.08 V versus Ag/AgCl, which can be assigned to the reduction of the nitro groups. On subsequent cycles, no current peak can be observed in the same voltage range. The reduction of the surface grafted nitro groups, occurs via a six-electron process for a complete conversion of one nitro to an amino group, as proposed by Allongue et al. (Scheme 2).[43,44]

(43) Vase, K. H.; Holm, A. H.; Pedersen, S. U.; Daasbjerg, K. *Langmuir* **2005**, *21*, 8085.
(44) Allongue, P.; Delamar, M.; Desbat, B.; Fagebaume, O.; Hitmi, R.; Pinson, J.; Savéant, J. M. *J. Am. Chem. Soc.* **1997**, *119*, 201.

Figure 6. (a) Cyclic voltammogram of an NB-functionalized UNCD electrode recorded in 100 mM potassium chloride aqueous electrolyte solutions. The first scan (1) shows an irreversible wave, peaking at −1.08 V vs Ag/AgCl, corresponding to the reduction of the residual nitro groups. (b) N1s core level XPS spectra of the NB-functionalized electrode before and after the electrochemical reduction. For comparison, a hydrogenated reference sample (bare UNCD) was recorded (dotted line).

Scheme 2. Electrochemical Reduction of the SAM of NB to the 4′-Amino-1,1-biphenyl (AB) SAM
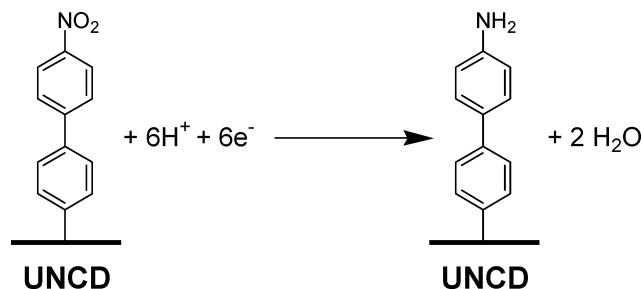
The charge, Q, associated with this redox process can be used to estimate the grafting density Γ of the NB monolayer:

$$\Gamma = \frac{Q}{n \cdot F \cdot A} = \frac{\int I \, dt}{n \cdot F \cdot A} \qquad (2)$$

Here, n is the number of electrons involved in the reduction, which is in this case $n = 6$. F is Faraday's constant, and A is the electrode area. For the depicted cyclic voltammogram in Figure 6a, the integrated charge is approximately 300 μC. Inserting this value into eq 2, a grafting density of $\Gamma = 5 \times 10^{-10}$ mol/cm^2 of a dense NB monolayer can be calculated, which is consistent with the XPS analysis.

The proposed electrochemical transformation of the nitro into the amino group of the NB SAM was also confirmed by XPS. In Figure 6b, the N1s region of a sample before and after electrochemical reduction is shown. The conversion fraction can be derived from the ratio of the two peak areas and yields approximately 60%. It should be noted that, although a full
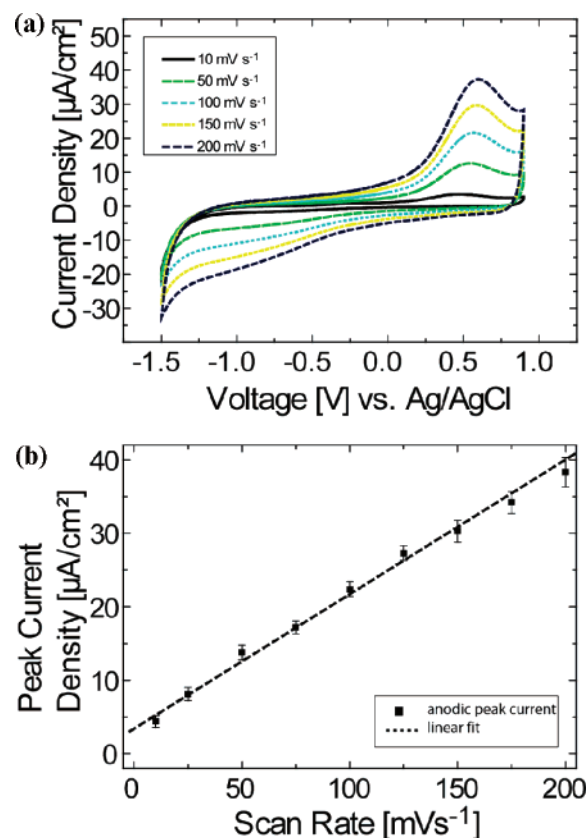
Figure 7. (a) Cyclic voltammograms of a reduced, NB-functionalized doped UNCD diamond electrode in 100 mM potassium chloride aqueous solution at various scan rates (10 to 200 mV s^{-1}). (b) Plot of the maximum anodic peak current density versus the scan rate.

conversion to NH$_2$ was not achieved, this value is still sufficient for the effective immobilization via consecutive surface reaction of small molecules, and especially of larger (bio-) polymers such as proteins or DNA. Furthermore, the possible in situ modification would allow a simultaneous measurement and thus a precise control of the surface grafting density.

Figure 7a contains a set of cyclic voltammograms of a reduced, functionalized UNCD electrode in 100 mM potassium chloride aqueous solution. An oxidation peak with a broadened reduction peak in the negative range of the scan is clearly visible. Increasing the scan rate causes the peak current to increase. The height of the anodic peak is directly proportional to the potential scan rate up to 200 mV/s (Figure 7b), indicating the presence of a surface-grafted redox group. The observed couple is assigned to the hydroxyaminobiphenyl/nitrosobiphenyl reversible interconversion as proposed by Brooksby and Downard.[45]

The reduction route can be divided in a first, irreversible chemical reaction followed by a second reversible step: First, the nitro group is not completely reduced and ends up in an electro-active intermediate state, as shown by the redox voltammograms in Figure 7a. Assuming a two-electron process, the integrated charge (20 μC) from the cyclic voltammogrammetry represents a surface coverage of approximately 1.0×10^{-10} mol/cm^2, up to 20% of the nitro group transform into a hydroxyamino. The nitroso groups or hydroxyl amino cannot be further converted into an amino group and could explain the presence of nitrogen with a chemical shift corresponding to

(45) Brooksby, P. A.; Downard, A. J. *L Langmuir* **2004**, *20*, 5038.

Scheme 3. Two-Step Reduction Route Found for the NB SAM on UNCD[a]
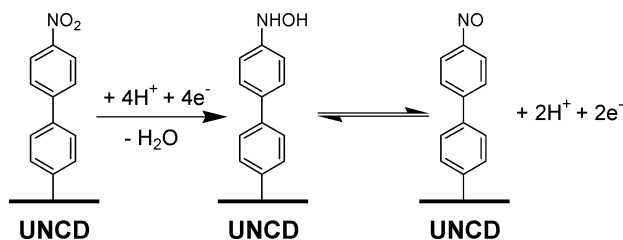
[a] First, a partial and irreversible electrochemical reduction of the NB to the 4′-hydroxyamino-1,1-biphenyl SAM occurs, followed by a reversible redox reaction between the hydroxyamino and nitroso species.

a N−O bond in the N1s XPS spectra of the converted electrode (Figure 6b). The route is summarized in Scheme 3.

Conclusion

We presented the formation and a detailed spectroscopic and electrochemical analysis of a chemical grafted SAM of NB on hydrogen-terminated UNCD surfaces. The SAM was formed by pure chemical grafting using the corresponding diazonium salt. Quantitative analysis by AFM, XPS, NEXAFS, and CV data have confirmed the presence of a densely packed monomolecular layer with a grafting density of $\Gamma = 4.5-5.3 \times 10^{-10}$ mol/cm^2, which calculates to a nominal area of $31-37$ Å^2/molecule. Comparing this to results of 4-methylmercapto-4-mercaptobiphenyl on gold,[46] where a density of 57.7 for a "lying-down" phase of the biphenyl moiety and 21.6 for the standing-up phase with a lower tilt angle, leads to the conclusion that the monolayer is densely packed, since our findings are based on macroscopic averaging quantification methods like CV and XPS. The layer thickness is corresponding to the molecular dimension of the NB molecule. The covalently grafted organic layer is hydrolytically stable and offers enhanced electron-transfer properties due to its conjugated aromatic structure. The

spontaneous grafting of aromatic molecules has important advantages as compared to other grafting processes such as electrochemical grafting: it is a milder functionalization method, which can be applied to pre-processed surfaces. In addition, the spontaneous grafting results in a homogeneous monolayer coverage, whereas electrochemical processes lead to multilayer formation in most of the cases.

We have also demonstrated the possibility of an electrochemically as well as X-ray irradiation-induced conversion of the terminal nitro function to the corresponding amine. The radiation-based transformation offers the possibility of X-ray lithography analogous to the chemical lithography using electron irradiation. By this, the direct creation of patterns with high chemical contrast is possible. This can be used for the patterned attachment of, for example, proteins or other biomolecules to create sensor arrays directly onto biocompatible diamond surfaces. In addition, the electrochemical conversion of the SAM offers the possibility of in situ coupling of proteins to the electrode surface in physiological environment. Currently, work is in progress to investigate further modifications of the aminated layers with inorganic redox probes as well as redox enzymes.

(46) Ulman, A. *Acc. Chem. Res.* **2001**, *34*, 855.

JA0657049